

Effect of Chromium on the Corrosion Behaviour of Low-Alloy Steels Containing Copper in FGD Environment

Sun Ah Park, Woo Soo Ji, Jung Gu Kim*

Department of Advanced Materials Engineering, Sungkyunkwan University; 300 Chunchun-Dong, Jangan-Gu, Suwon 440-746, South Korea

*E-mail: kimjg@skku.ac.kr

Received: 13 April 2013 / Accepted: 7 May 2013 / Published: 1 June 2013

The effects of chromium addition on the corrosion resistance of low alloy steels containing copper in FGD systems, were examined by electrochemical techniques in a sulphuric acid solution containing HCl. All measurements (potentiodynamic polarization test and EIS) reveal an increase in corrosion rate with Cr content, confirming the deterioration of corrosion resistance by Cr addition. EPMA, XPS and SEM examinations of the corroded surface indicated that the addition of chromium increased corrosion damage to the steels by microgalvanic corrosion between a grain as an anode and a grain boundary as a cathode because Cu-containing steel increases the tendency to chromium segregation at grain boundaries.

Keywords: Low-alloy steel; Corrosion; Sulphuric acid; EIS; Polarization

1. INTRODUCTION

The removal of polluted gases from the exhaust produced by the combustion of fossil fuels is carried out by flue gas desulphurization systems (FGDs). The heat and chemical products influence the steels that make up the power plant. When the temperature of the exhaust gas falls to the dew point, the sulphur oxides and H₂O in the gas react to form highly concentrated sulphuric acid which causes steel to corrode. This phenomenon is called sulphuric acid dew point corrosion. Under these conditions, the low-alloy steels were confronted with a serious corrosion environment, in which concentrated H₂SO₄ absorbed HCl at 60~70 °C [1-2].

Weathering steels containing Cu, Ni, Co, and Sb have been widely used on account of their excellent atmospheric corrosion resistance[3-4]. However, these weathering steels do not have good corrosion resistance in the FGD environment. To improve their corrosion resistance in these severe conditions, various elements were alloyed with the weathering steel base metal. High-nickel alloys and

stainless steels were often more resistant to the FGD environment but were usually not economically competitive with carbon steel and cast irons. Above all, the addition of chromium has been widely used to enhance the corrosion resistance of weathering steel. Steels alloyed with chromium exhibit enhanced corrosion resistance in sulphuric acid solution by forming a passive film on their surfaces. The protective properties of the passive film in H_2SO_4 or chloride-containing H_2SO_4 solution were improved by the addition of chromium[5-7].

The purpose of this study is to investigate the effect of chromium on the corrosion resistance of low-alloy steels in a concentrated sulphuric acid solution containing HCl by using electrochemical methods (potentiodynamic polarization test and EIS) and surface analyses (EPMA, SEM, XPS).

2. EXPERIMENTAL PART

2.1. Materials and test conditions

Low alloy steels containing 0.07 C, 0.25 Si, 0.7 Mn, 0.05 Co, 0.01 S, 0.35 Cu, and different chromium concentrations (0.00; 0.50 Cr) were used. The specimens were cut into 15 mm×15 mm pieces for the electrochemical test. The specimen was ground with 800-grit silicon carbide (SiC) paper, degreased in an ultrasonic cleaner with ethanol for 5 min, followed by cleaning with distilled water and drying in hot air. All of the electrochemical tests were carried out in 1000 ml of a solution containing 16.9 vol. % H_2SO_4 + 0.35 vol. % HCl at 60°C. To ensure the reproducibility of the results, at least three measurements were performed for each specimen.

2.2. Electrochemical measurements

The electrochemical tests consisted of potentiodynamic polarization and EIS tests which were conducted in a three-electrode electrochemical system. A saturated calomel electrode (SCE) and two pure graphite rods were used as the reference and the counter electrodes, respectively. A stable open-circuit potential (OCP) was established within 1 h before each electrochemical measurement.

The potentiodynamic polarization test was performed to evaluate the overall corrosion behaviour of the specimens. All of the specimens were allowed to stabilize in the solution for 1 h. The potential of the electrode was swept at a rate of 0.166 mV/s from the initial potential of -250 mV versus OCP to the final potential of +100 mV.

After the specimen reached the stable OCP, EIS measurements were obtained with an amplitude of 20 mV in the frequency range from 100 kHz to 10 mHz. Then, to obtain a better understanding of the effect of chromium on the corrosion behaviour, the EIS tests were performed for the duration of 6 hours at an interval of 1 hour.

2.3. Surface analyses

To investigate the relationship between the alloying element and the surface morphology of the corrosion products, the surface was examined using X-ray photoelectron spectroscopy (XPS) after 6 h

of immersion. The corroded surface features after polarization tests and various immersion times were inspected by scanning electron microscopy (SEM).

3. RESULTS AND DISCUSSION

3.1. Potentiodynamic polarization test

The potentiodynamic polarization test was undertaken to examine the electrochemical behaviour of the low alloy steels and establish a baseline for the experimental data. Figure 1 illustrates the potentiodynamic polarization curves of 0% Cr, 0.5% Cr low-alloy steels. All of the curves exhibited active corrosion behaviour, indicating that the anodic current density increases continuously with increasing potential. This is because a protective rust film does not form on the surface. The anodic current density was increased due to Cr addition, confirming the deterioration of corrosion resistance by Cr addition.

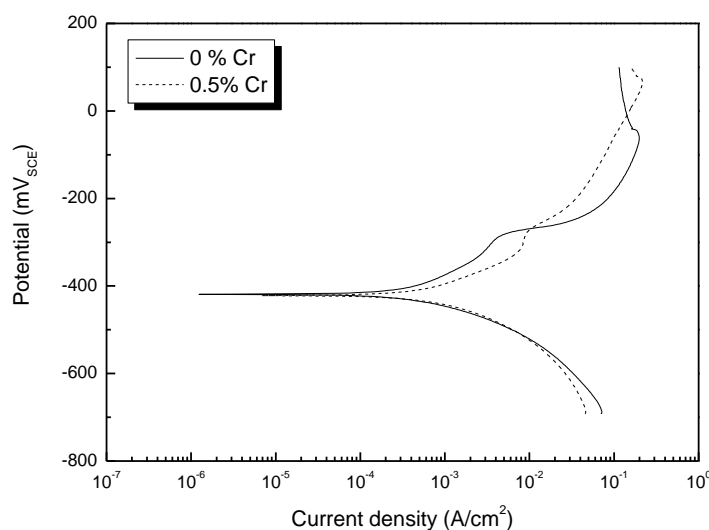


Figure 1. Potentiodynamic polarization curves of specimens in 16.9 vol. % H_2SO_4 + 0.35 vol. % HCl at 60°C .

The corrosion rates were calculated by the Tafel extrapolation method. Based on Faraday's law, the corrosion current density is measured and can yield the corrosion rate[8]:

$$\text{Corrosion rate (mm/y)} = 3.16 \times 10^8 i_{\text{corr}} M / zF\rho \quad (1)$$

where i_{corr} is the corrosion current density (A/cm^2), M is the molar mass of the metal (g/mol), z is the number of electrons transferred per metal atom, F is Faraday's constant, and ρ is the density of the metal (g/cm^3). Using the anodic reaction for Fe as an example, $\text{Fe} = \text{Fe}^{2+} + 2e^-$, two equivalents are transferred for each atomic weight reacted. Table 1 summarizes the potentiodynamic polarization data, highlighting the detrimental effects of Cr.

Table 1. Electrochemical parameters of potentiodynamic polarization measurements in 16.9 vol. % H₂SO₄ + 0.35 vol. % HCl at 60 °C.

| Specimen | E _{corr} | i _{corr} | β _a | β _c | Corrosion rate (mm/year) |
|----------|-------------------|----------------------|----------------|----------------|-----------------------------|
| | (mV) | (A/cm ²) | (V/decade) | (V/decade) | |
| 0Cr | -425.7 | 0.00186 | 0.099 | 0.1811 | 21.53 |
| 0.5Cr | -432.9 | 0.00692 | 0.1941 | 0.2058 | 80.24 |

3.2. Electrochemical impedance spectroscopy (EIS)

EIS has the capability to give valid measurements of polarization resistance and corrosion rate which are corrected for ohmic interferences from the solution resistance. Figure 2 presents the Nyquist plots of the specimens. The high-frequency capacitive loop in the Nyquist plot is related to the rust layer on the surface and the low-frequency capacitive loop is related to the charge transfer process. As presented in Figure 2, the impedance spectra measured from the specimens show a single semicircle. Therefore, a general equivalent circuit is proposed in Figure 3[9]. The equivalent circuit consists of a solution resistance (R_s), capacitance (C_{dl}), and a charge-transfer resistance (R_{ct})[10]. During the fitting process, the capacitance was represented by a constant phase element (CPE) to allow for the depressed semicircles.

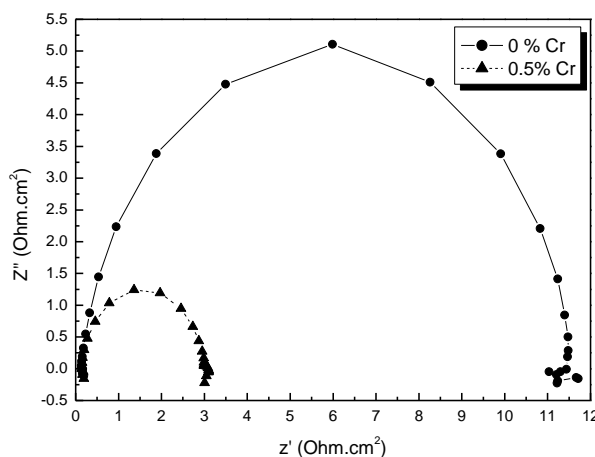


Figure 2. Nyquist plots of specimens in 16.9 vol. % H₂SO₄ + 0.35 vol. % HCl at 60°C.

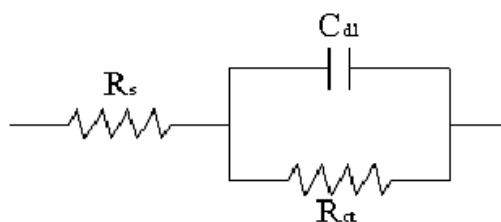


Figure 3. Equivalent circuit used to fit EIS data.

The EIS results were fitted according to this proposed equivalent circuit for the specimens by Zsimpwin and are presented in Table 2. The corrosion rates of the specimens were obtained from the corrosion current density. The corrosion current density was calculated by using the following equation:

$$R_{ct} = \beta_a \beta_c / 2.3i_{corr}(\beta_a + \beta_c) \quad (2)$$

It was assumed that the values of β_a and β_c are equal to 0.1 V/decade in this case. The results of the EIS measurement showed that the addition of chromium increased the corrosion rates of the specimen.

Table 2. Impedance parameters of specimens in 16.9 vol. % H₂SO₄ + 0.35 vol. % HCl at 60 °C.

| Specimen | R _s (Ωcm ²) | C _{dl} (F/cm ²) | R _{ct} (Ωcm ²) | i _{corr} (mA/cm ²) | Corrosion rate (mm/year) |
|----------|---------------------------------------|---|--|--|-----------------------------|
| 0Cr | 0.1763 | 3.566E-4 | 11.36 | 1.91 | 22.20 |
| 0.5Cr | 0.1977 | 2.517E-4 | 2.80 | 7.78 | 90.23 |

Figure 4 illustrates the Nyquist plots as a function of the immersion time for the specimens. The diameter of the arc first decreased and then increased with increasing immersion time. These results indicated that a stable rust layer was not formed on the steel surface during the initial period of immersion. Figure 5 shows the corrosion rates of the specimens as a function of the immersion time. After some hours, the corrosion rates decreased slightly because the surface of the steels was covered with corrosion products.

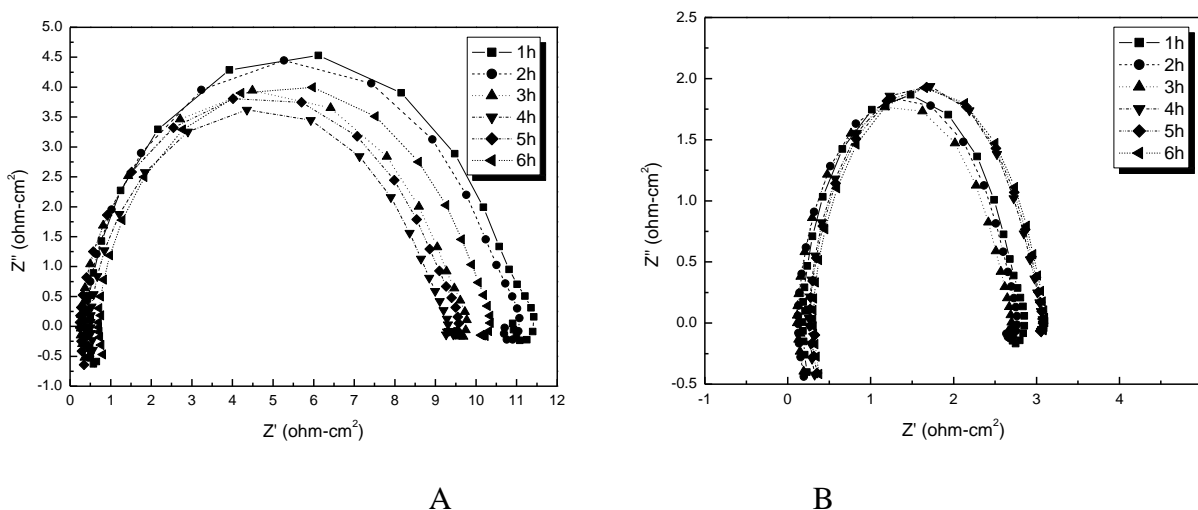


Figure 4. Nyquist plots of specimens as a function of the immersion time: (a) 0% Cr, (b) 0.5% Cr.

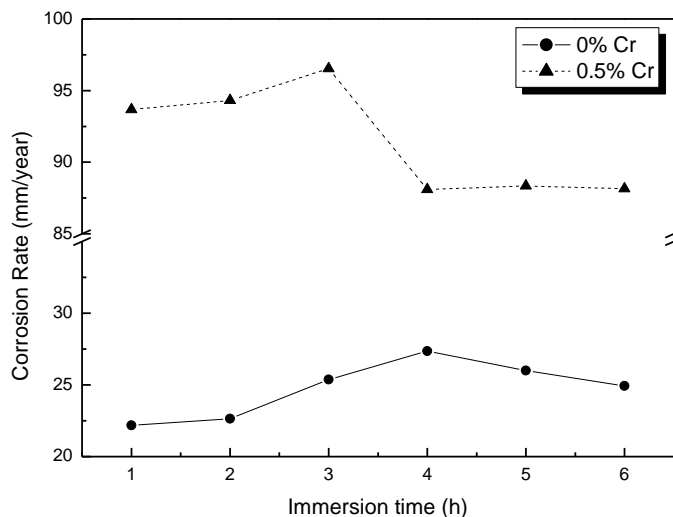
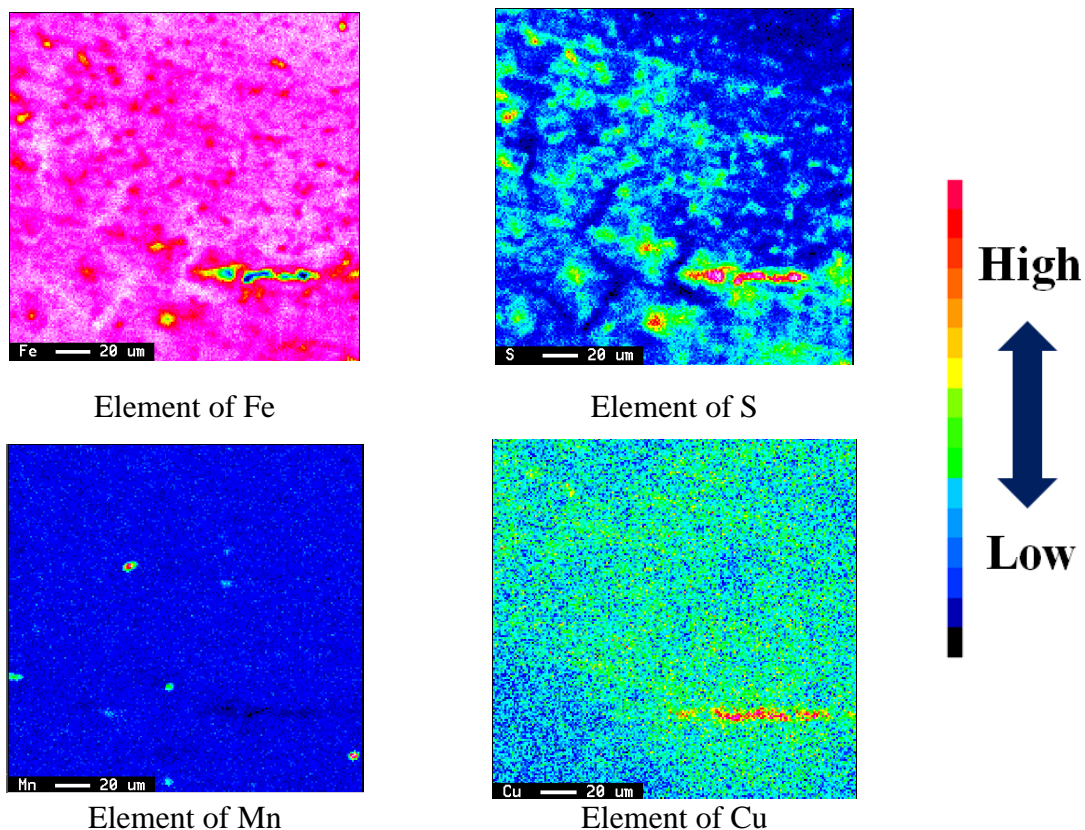


Figure 5. Corrosion rates of the specimens as a function of the immersion time.

3.3. Surface analyses

Figure 6 shows the mapping images of the specimens produced by EPMA after 6 h of immersion. As the chromium was added, Mn, S, Cu and Cr became more localized after the electrochemical tests. Particularly, as shown in Figure6 (b), some parts of chromium and copper were replaced by sulphur.



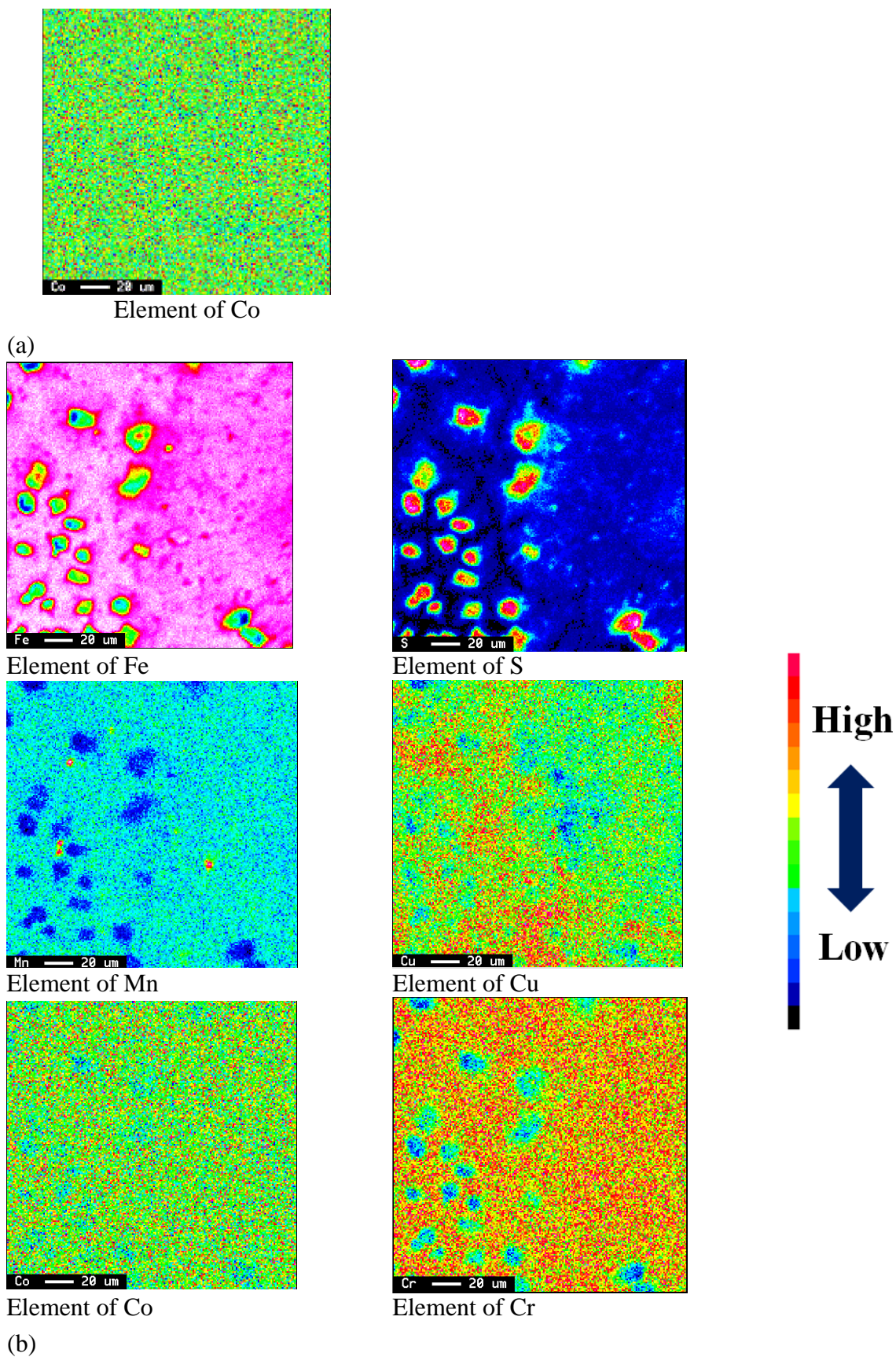
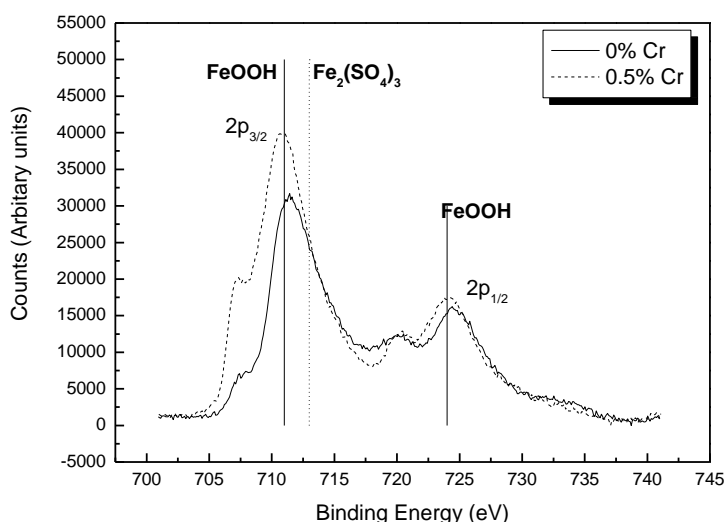


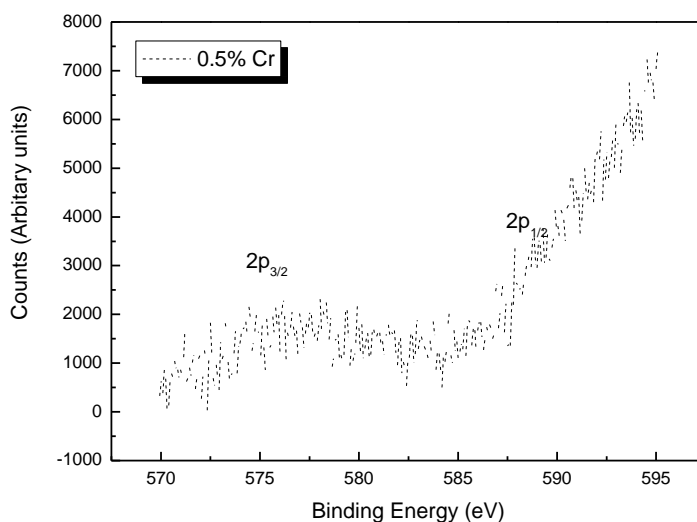
Figure 6. EPMA mapping results of the specimens after the 6 hour EIS tests: (a) 0% Cr, (b) 0.5% Cr.

After 6 h of immersion in 16.9 vol. % H₂SO₄ + 0.35 vol. % HCl at 60 °C, the corrosion products on the surface were examined by XPS. Figure 7 shows the results of the XPS analyses. As seen in the Figure 7, the spectra of iron consisted of Fe₂(SO₄)₃ and FeOOH. The dissolved Fe²⁺ from the substrate formed iron oxides such as Fe₂(SO₄)₃ and FeOOH on the surface of steels. The steels containing chromium had higher spectra of iron than the steel without chromium. The spectra of chromium show that the specimens containing chromium did not form any chemical compounds on the surface. Generally, the addition of chromium leads to the formation of passive layers such as Cr₂O₃ or Cr(OH)₃ on the surface in sulphuric acid. However, the addition of chromium does not contribute to the formation of any passive films in 16.9 vol. % H₂SO₄ + 0.35 vol. % HCl at 60 °C.

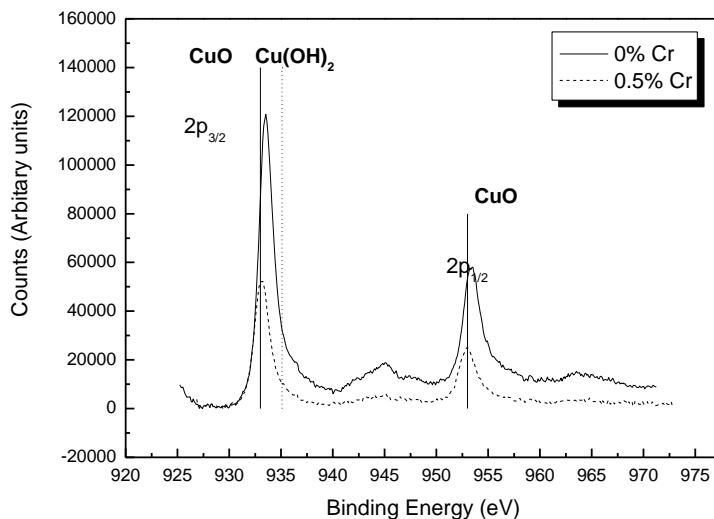
In the case of the copper spectra, the steel without chromium had a higher spectrum of copper than steels containing chromium.



(a)



(b)

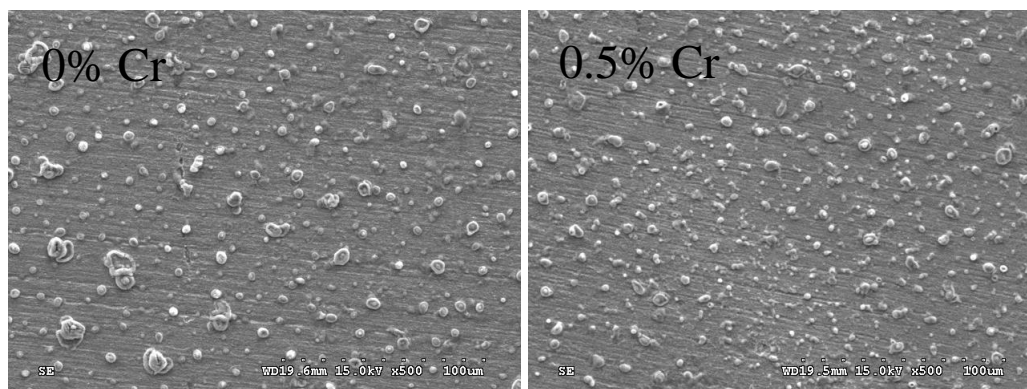


(c)

Figure 7. XPS spectra of alloying elements from the rust of the specimens: (a) Fe peaks, (b) Cr peaks, (c) Cu peaks.

The corrosion products formed on the surfaces of the steels were composed of copper oxides such as CuO and Cu(OH)₂[11]. It was thought that the addition of chromium inhibited the formation of copper oxides on the surface.

Figure 8 shows the SEM images of the 0% Cr and 0.5% Cr specimens after various immersion times. Initially, pits were initiated locally and then these pits expanded due to microgalvanic corrosion. The pits of the 0.5% Cr specimen were more severe than those of the 0% Cr specimen. Moreover, the pits of the 0.5% Cr specimen expanded and deepened with increasing immersion time. Figure8-(d) showed that the 0% Cr and 0.5% Cr specimens changed their corrosion patterns from localized corrosion to uniform corrosion. Finally, corrosion patterns of 0.5% Cr specimen consisted of a combined pattern (pitting corrosion + uniform corrosion)[12-13]. Localized corrosion is caused by continuous stringers of non-metallic inclusions. However, it has been pointed out that localized corrosion has occurred in steel without any stringers of non-metallic inclusions. Therefore, the segregation of some alloying element might cause localized corrosion[14].



(a)

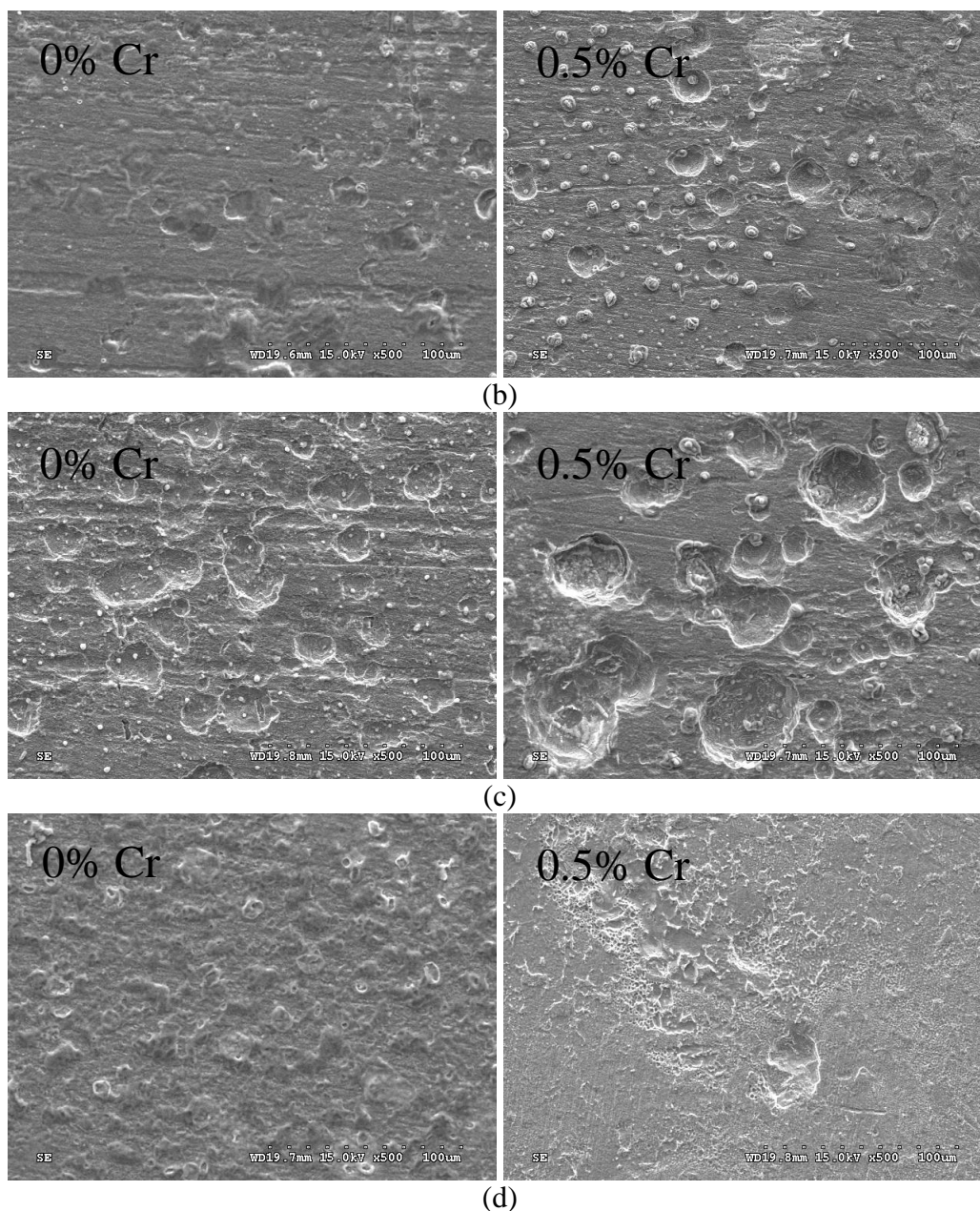


Figure 8. SEM analyses of 0% Cr and 0.5% Cr-containing steels after various immersion times: (a) after 10 min., (b) after 20 min., (c) after 30 min., (d) after 45 min.

Copper addition in steel increases the tendency to chromium segregation at grain boundaries[15]. Localized corrosion was by the galvanic action between a grain as an anode and a grain boundary as a cathode[14]. It was thought that these localized segregation of Cr alloying element accelerated the pitting corrosion and thus increased the corrosion rate.

The mechanism of the localized corrosion by Cr segregation of low alloy steel in a strong acid solution is shown in Figure 9. The process split into four steps ; (1) Copper addition in steel increases the tendency to chromium segregation. (2) Localized corrosion was caused by preferential corrosion of a low-chromium part. Fe, Cr dissolves to Fe^{2+} , Fe^{3+} , Cr^{3+} , ions in a strong acid solution. Especially, Cu dissolves to Cu^{2+} ions by reduction of the dissolved oxygen. (3) Cu^{2+} in a Fe, H_2O and O_2 system acts as an oxidant to the Fe. Therefore, a proportion of the Cu^{2+} will reduce and then re-deposit onto the

substrate through a reduction reaction (consumption of the electrons produced by oxidation of the Fe)[9]. (4) The re-deposited Cu will be precipitated as re-crystallized Cu oxides on the already formed uneven surface by preferential corrosion of a low-chromium part.

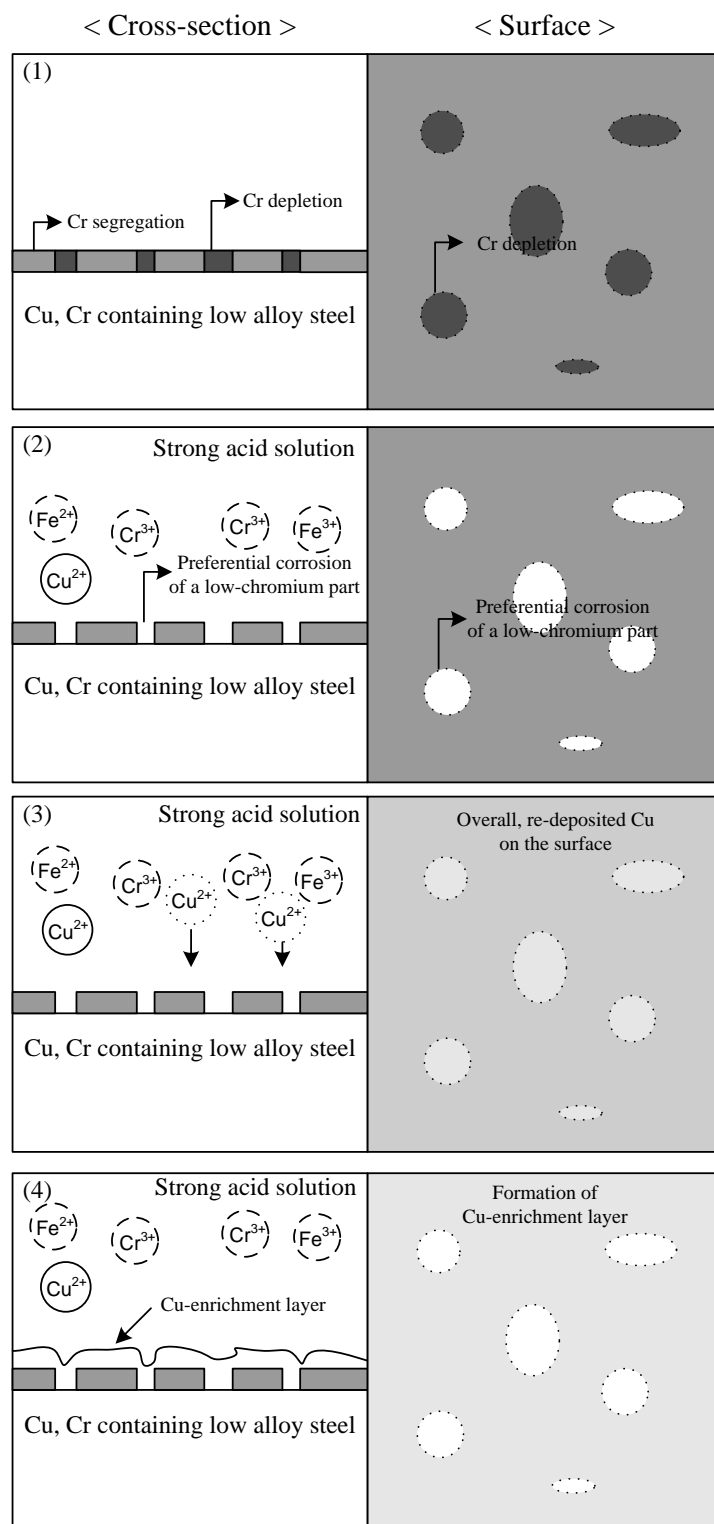


Figure 9. Schematic diagrams of the localized corrosion by Cr segregation of Cu, Cr containing low alloy steel in a strong acid solution.

4. CONCLUSIONS

1. None of the specimens showed passive behaviour in 16.9 vol. % H₂SO₄ + 0.35 vol. % HCl at 60 °C. They all exhibited active corrosion in this solution. As the content of Cr was increased, the corrosion rate increased.
2. The addition of chromium increased localized corrosion by microgalvanic couple between a grain as an anode and a grain boundary as a cathode due to the chromium segregation at grain boundaries.
3. The addition of 0.5% Cr inhibited the formation of copper oxides on the surface.

ACKNOWLEDGMENTS

This study was supported by the Korea Ministry of Knowledge Economy through the Strategic Technology Development Program.

References

1. U. Akira, O. Motohiro, S. Shunji, *Nippon. Steel. Tech. Rep.*, 90 (2004) 25
2. F. Ferrer, T. Faure, J. Goudiakas, E. Andres, *Corros. Sci.*, 44 (2002) 1529
3. J. C. Hudson, J.F. Stanners, *J. Iron Steel Inst.*, 180 (1955) 271
4. C. P. Larrabee, S. K. Coburn, *Proceedings of the 1st International Congress on Metallic Corrosion*, Butterworths, London (1961)
5. L. Wann-Chiu, C. Wen-Chi, W. Jiann-Kuo, *Mater. Lett.*, 59 (2005) 3295
6. A. A. Aksut, A. N. Onal, *Corros. Sci.*, 39 (1997) 761
7. A. A. Hermas, M. Nakayama, *Electrochim. Acta.*, 50 (2005) 3640
8. D. A. Jones, *Principles and Prevention of Corrosion*, Prentice Hall, Upper Saddle River, New Jersey (1996)
9. J. H. Hong, S. H. Lee, J. G. Kim, *Corros. Sci.*, 54 (2012) 174
10. R. Cottis, S. Turgoose, *Electrochemical Impedance and Noise*, NACE, Houston (1999).
11. W. M. Skinner, C. A. Prestidge, R. St. C. Smart, *Surf. Interface Anal.*, 24 (1996) 620
12. T. Akira, S. Tadashi, *Corros. Sci.*, 47 (2005) 2589
13. G. Wranglen, *Corros. Sci.*, 14 (1974) 331
14. H. Kajimura, M. Harada, T. Okada, M. Okubo, H. Nagano, *Corrosion*, 51 (1995) 507
15. J. Banas, A. Mazurkiewicz, *Mat. Sci. Eng.*, A 277 (2000) 183